PREDICTING THERMAL SHAPE MEMORY OF CROSSLINKED POLYMER NETWORKS FROM LINEAR VISCOELASTICITY

Julie Diani[a,*], Pierre Gilormini[a], Carole Frédy[a], Ingrid Rousseau[b]

[a] PIMM, CNRS, Arts et Métiers ParisTech, 151 bd de l'Hôpital, 75013 Paris, FRANCE.

[b] General Motors Company, Research & Development Center, 30500 Mound Rd, Warren, MI 48090-9055, USA.

[*] Corresponding author: julie.diani@ensam.eu, tel: +33 1 44 24 61 92, fax: +33 1 44 24 62 90.

ABSTRACT:

The viscoelastic behavior of an amorphous shape-memory polymer network and its dependence on time and temperature were measured by dynamic mechanical analysis. The resulting thermo-mechanical behavior was modeled and implemented in a commercial finite element code. The ability of the resulting thermomechanical model to simulate and, eventually, predict the shape storage and shape recovery of the material was evaluated by comparison with experimental shape memory thermomechanical torsion data in a large deformation regimen. The simulations showed excellent agreement with experimental shape memory thermomechanical cycle data. This demonstrates the dependence of the shape recovery on time and temperature. The results suggest that accurate predictions of the shape recovery of any amorphous polymer networks under any thermomechanical conditions combination solely depends on considering the material viscoelasticity and its time-temperature dependence.

Keywords: Shape-memory, Polymers, Modelling, Thermomechanical, Viscoelastic, Finite element

1. Introduction

The shape memory property of polymers has drawn a substantial amount of interest among the mechanical modeling community during the past decade. Two approaches are commonly described in the literature for the modeling of the thermomechanical behavior of shape memory polymers (SMPs). The first type is purely elastic and describes an amorphous crosslinked shape memory polymer as a two-phase material composed of a glassy phase and a rubbery phase. Hence, a model

is required that combines the stiffness of each phase to predict that of the two-phase composite material. This can be done in various ways. Such an approach has been proposed by Liu et al. (2006), Chen and Lagoudas (2008a), and Wang et al. (2009). Chen and Lagoudas (2008b) included an extension to finite strain, while Reese et al. (2010) implemented a variant of the model using finite element analysis to simulate the deformation of a stent. Recently, Gilormini and Diani (2012) underlined that such purely elastic theories also provide the thermal expansion of the two-phase material, and a comparison with experimental results invalidates the uniform stress assumption that is used in most papers cited above. Moreover, the volume fraction of each phase in such models must be given as a function of temperature and is obtained from fitting the experimental shape memory data. As a result, such models can eventually simulate but cannot predict the shape-memory response of a material under varying heating rates or heating profiles such as for instance, heating and maintaining the material to intermediate temperatures between the low (i.e., fixing temperature) and the high (deformation) temperatures used for shape memory programming. The other approach that can be used to describe the thermomechanical behavior of SMPs uses the viscoelastic properties of polymers. Under more or less complex forms for various types of shape-memory polymers (not only amorphous thermosets), this approach has been adopted by Tobushi et al. (1997), Lin and Chen (1999), Morshedian et al. (2005), Diani et al. (2006), Hong et al. (2007), Nguyen et al. (2008), Srivastava et al. (2010), Heuchel et al. (2010), amongst others. Note that intermediate models to the two approaches above were described by Qi et al. (2008) and by Xu and Li (2010) who defined a two-phase viscoelastic mixture.

The set of viscoelastic models chosen above illustrates the large variety of approaches employed in the literature to simulate and predict the shape memory behavior of materials. Some require the fitting of parameters on experimental shape-memory data to determine either the mechanical behavior (Tobushi et al. 1997, Morshedian et al 2005, Diani et al. 2006, the 3D variant of Heuchel et al., 2010) or volume fraction (Qi et al. 2008, Xu and Li 2010), whereas others rely on series of standard tension or compression tests at constant stress (Lin and Chen 1999, Hong et al. 2007) or constant strain rate (Srivastava et al. 2010). Finally, most models are unidimensional and compared with uniaxial shape-memory experiments only (Tobushi et al. 1997, Lin and Chen 1999, Morshedian et al. 2005, Hong et al. 2007) and few are general complex 3D models (Nguyen et al. 2008) with capabilities far beyond the shape memory effect (Srivastava et al. 2010). Despite these differences, all models, except for the one by Hong et al. 2007, who uses 8, include a small number (one or two) of Maxwell branches which may be a reason for some of the discrepancy between the measured and predicted shape memory behavior. This point is revisited in the present paper. Note that the most elaborate model, such as that introduced by Srivastava et al. (2010), gives the best, although

imperfect, agreement. None of these models relies on dynamic mechanical analysis tests conducted systematically over a wide range of temperatures and frequencies to identify the parameters involved. When the number of material parameters is large, more than 18 in Hong et al. (2007) and up to 45 in Srivastava et al. (2010) for instance, they are obtained either from standard curve fitting procedures (Hong et al., 2007) or through a specific complex calibration process (Srivastava et al., 2010).

The original approach described herein is based solely on viscoelasticity. The influence of thermal conditioning as described above during shape recovery is intrinsically included. There is no need for shape memory cycling experiments to fit any of the model parameters. The time-temperature dependence of the viscoelastic properties of the polymers is determined using a well known dynamic mechanical analysis procedure which becomes the sole requirement for the model proposed herein to accurately predict the shape memory behavior of the material and, more interestingly, its shape recovery and recovery time-temperature dependence.

Here, a standard finite element code was used to simulate a series of shape memory torsion tests. The simulation results reproduced precisely and accurately experimental shape memory torsion tests simply by assuming the amorphous shape memory thermoset to behave as a thermorheologically simple generalized Maxwell model. Because torsion tests involve non-homogeneous strains and stresses, they shall provide a better validation than the standard shape memory uniaxial tension or compression tests commonly reported in the literature. Moreover, torsion tests enable the polymer to reach large deformations, i.e., with large displacements and rotations involved, with moderate strains, which are believed to be more representative of SMP application requirements. A benefit of the proposed model lies in its ability to simulate *and* predict the shape recovery of thermally activated shape memory polymers solely using their known intrinsic thermoviscoelastic properties without having to introduce any adjustable parameters based on shape-memory data fitting or other. Furthermore, the model implementation is based only on a combination of standard features from commercially available finite element codes and does not call for the contribution, hence development, of any additional elaborated routines. In turns, the proposed model shall allow designing shape memory polymer parts with large deformation requirements, such as stents and deployable structures, based on its prediction results of the shape memory response of polymers with varying composition, structure, and geometry, and under varying thermomechanical cycling conditions.

2. Materials and experiments

2.1. Materials

The epoxy network (epoxy 12DA3) was synthesized by reacting a bisphenol-A-based epoxy monomer (Dow D.E.R. 383) with a diamine crosslinker (Jeffamine D-230) and a monoamine (N-decylamine). Dow D.E.R. 383 (diglycidyl ether of bisphenol-A, DGEBA) was purchased from the Dow Chemical Company. Jeffamine D-230 ((propylene glycol)bis(2-aminopropyl)) was obtained from the Huntsman company. N-decylamine was purchased from Aldrich. All chemicals were used as received. Stoichiometric molar ratios of the amine to epoxy monomers were used to reach a relative composition of 72.4 wt-% of Dow D.E.R. 383, 5.4 wt-% of Jeffamine D-230, and 22.2 wt-% of N-decylamine. The reactants were added and mixed manually in their order of lower to higher volatility. Once thoroughly mixed the solution was degassed at room temperature prior to being injected inside a glass mold previously coated with a mold release agent (ChemLease 5037 from ChemTrend). The curing reaction was initiated after the mold was sealed and placed in a conventional oven. The following curing thermal program was followed: (i) heating to 100°C, (ii) holding isothermally at 100 ^{o}C for one hour, (iii) heating to 125°C, and (iv) holding isothermally at 125 ^{o}C for one hour. Upon completion of the thermal program the epoxy plaques were allowed to cool slowly in the oven before being removed from the glass mold. The cured epoxy plaques obtained had an average thickness of 1.6 mm.

2.2. Linear viscoelastic tests

The epoxy was tested in dynamic mechanical analysis (DMA) using rectangular samples cut from the material plates to the final dimensions 1.6 mm x 11.75 mm x 40 mm. DMA tests were run on a RDA III Rheometric Scientific® torsion rheometer.

The glass transition temperature range was first determined by testing the sample using a 2 °C/min dynamic temperature sweep at 0.2% strain and 1 Hz (Figure 1). At 1 Hz, the material changes from its glassy state to its rubbery state through a wide temperature range that extends approximately from 38 °C to 70 °C.

The time-temperature dependency of the viscoelastic properties of the material were determined using dynamic frequency sweeps at 0.2% strain for frequencies ranging from 0.01 to 63 Hz. The temperature was increased stepwise from 40 °C to 60 °C with 5 °C temperature increments. Figure 2 shows the material temperature-dependent viscoelastic properties. By applying the time-temperature superposition principle, the values of the storage modulus and of the loss angle (tan δ) as a function of frequency (alternatively temperature) can be obtained for an otherwise not measurable wide range of frequencies (alternatively temperature). Such master curves are shown in

Figure 3 where the reference temperature was selected as T_{ref} = 50 °C (peak of tan δ from the dynamic temperature sweep test at 1 Hz). The horizontal shift factor values $log_{10}(a_T)$ obtained using this time-temperature superposition were found to obey the Williams-Landel-Ferry (WLF) equation (Williams et al., 1955):

$$1/log_{10}(a_T) = \frac{-1}{C_1} - \frac{C_2}{C_1}\frac{1}{T-T_{ref}} ,$$

where C_1=10.17 and C_2= 47.35 °C with T_{ref} = 50 °C (see inset in Figure 3).

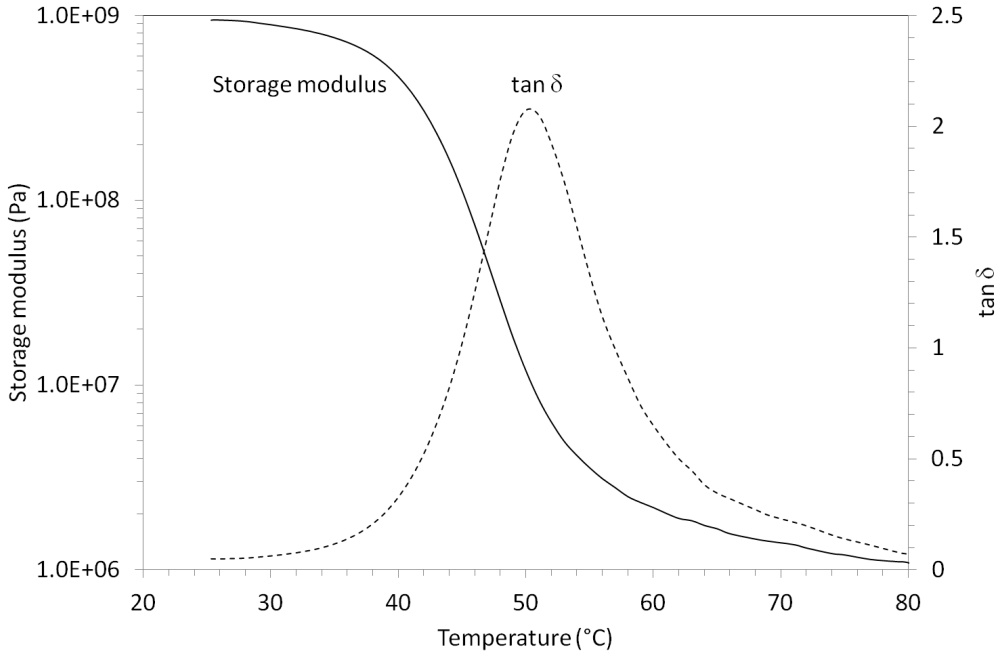

Fig. 1. DMA data of the epoxy obtained from a temperature sweep test at 2 °C/min, 0.2% strain and 1 Hz.

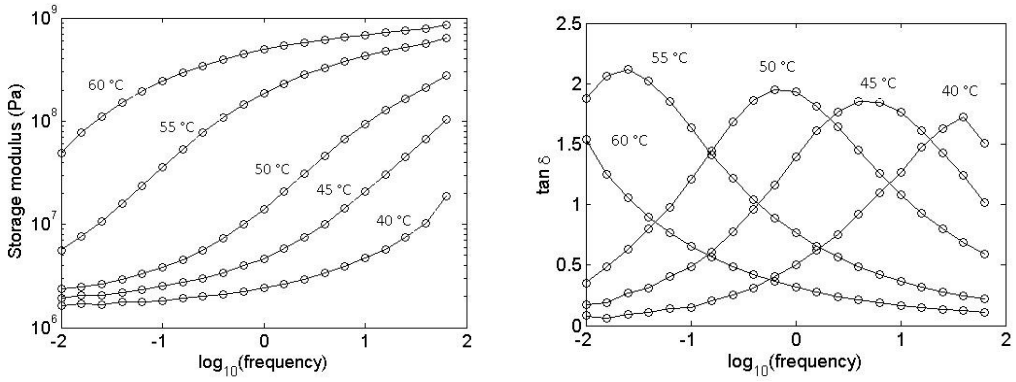

Fig. 2. Epoxy storage modulus and tan δ as a function of frequency under varying isothermal conditions as measured from DMA tests.

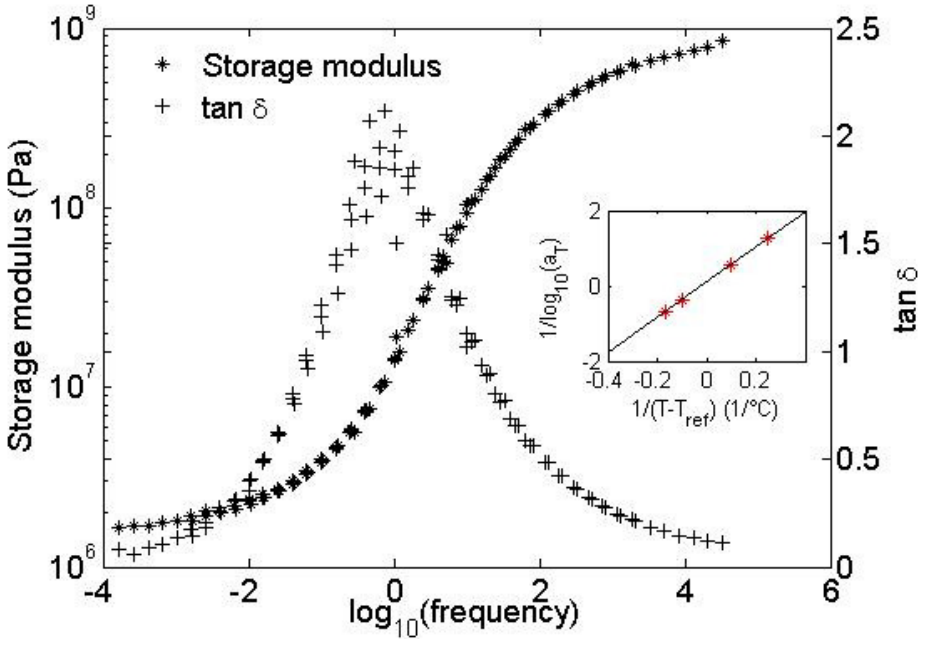

Fig. 3. Storage modulus and tan δ master curves of the epoxy obtained from horizontal shifting of the experimental data shown in Figure 2 using a reference temperature of 50 °C. The inset shows the WLF approximation (solid line) of the calculated horizontal shift factors.

2.3. Large deformation shape recovery test

A torsion device was built to test the large deformation shape recovery of polymers (Diani et al., 2011). The thermomechanical test consists in 5 steps: 1) A slender rectangular sample (100 mm x 10 mm x 1.6 mm, clamped over 5 mm at each end) is heated above its glass transition temperature, T_g (i.e., shape memory transformation temperature), 2) The sample is submitted to a torsion of 360 degrees, 3) The torsion angle is maintained while the material is cooled below T_g, 4) Stresses are released and the deformation that remains due to restrained molecular mobility below T_g characterizes the shape fixity of the material, 5) The torsion angle recovery is measured while heating the sample.

The temperature was recorded on a control sample positioned next to the sample being tested. To check for temperature homogeneity along the slender sample, the temperature was measured at 3 locations: at both extremities and at the length midpoint.

In step 3, the material was cooled at an average rate of -2 °C/min, which was not varied due to its limited effect on the shape recovery of SMPs (Castro et al., 2010). In step 4, an elastic recovery of less than 1° was generated from releasing the external stress. This excellent shape fixity (R_f >359/360 (99.7%) of the material at low temperature, below T_g, is consistent with the value (99.8%) given by the estimate R_f=1-G_e/G_g obtained readily for simple shear, when the rubbery modulus G_e and glassy

shear modulus G_g given in Section 3 are used. To emphasize the viscoelastic nature and time-temperature dependence of the shape recovery property, various heating histories were tested in step 5. The material was heated up to a high temperature largely above the glass transition at a constant heating rate. This is the most common test encountered in the literature. The effect of heating rate on shape recovery was evaluated using three heating rates (1.1 °C/min, 3.2 °C/min and 5.6 °C/min). Or, the material was heated up to an intermediate temperature of 42 °C, within the glass transition, and maintained at this temperature while shape recovery proceeded. This test will be referred to herein below as 'ramp-stop' test. Since at 42 °C the material is merely crossing its glass transition (Figure 1), a slow shape recovery is expected in this case.

Figure 4 shows the measured torsion angle recovery as a function of temperature under varying heating rates. The material exhibited complete shape recovery. As expected (Rousseau et al. 2010), the shape recovery varied with heating rates so that the recovery process initiated at higher temperatures for faster heating rates. Similar results were observed by Castro et al. (2010) during uniaxial tests performed on a different shape-memory polymer. Figure 5 presents the torsion angle recovery as a function of time for the ramp-stop test when the sample was heated to 42 °C and held isothermally. One can see that the shape recovery continued when temperature was held constant at 42 °C, which highlights the relationship that exists between time, temperature and shape recovery for the amorphous polymer network, which could not be predicted from the purely elastic models reported by other studies and discussed above to describe the shape memory effect.

The following section aims at showing that this relationship can be obtained from simple DMA tests. For this purpose, the epoxy thermoelastic behavior was modeled using the time-temperature superposition principle and a generalized Maxwell model. The thermomechanical behavior was then input in the Abaqus finite element code to predict the torsion shape memory response of the material, thereby replicating the experimental shape memory tests.

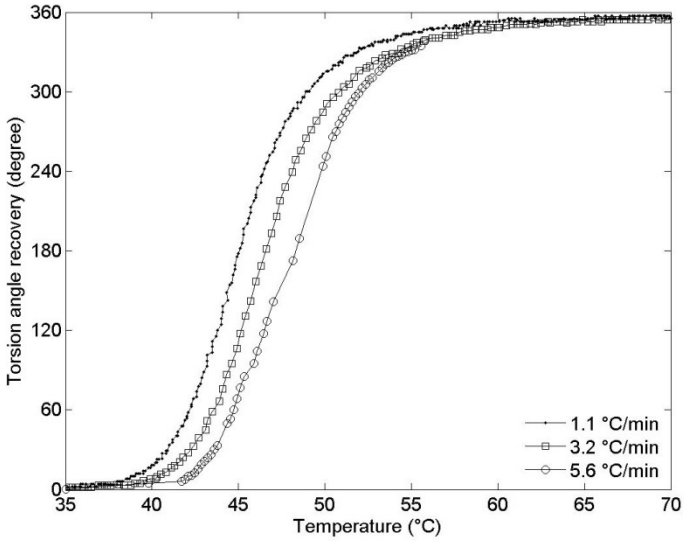

Fig. 4. Torsion shape recovery of the epoxy as a function of temperature for various heating rates.

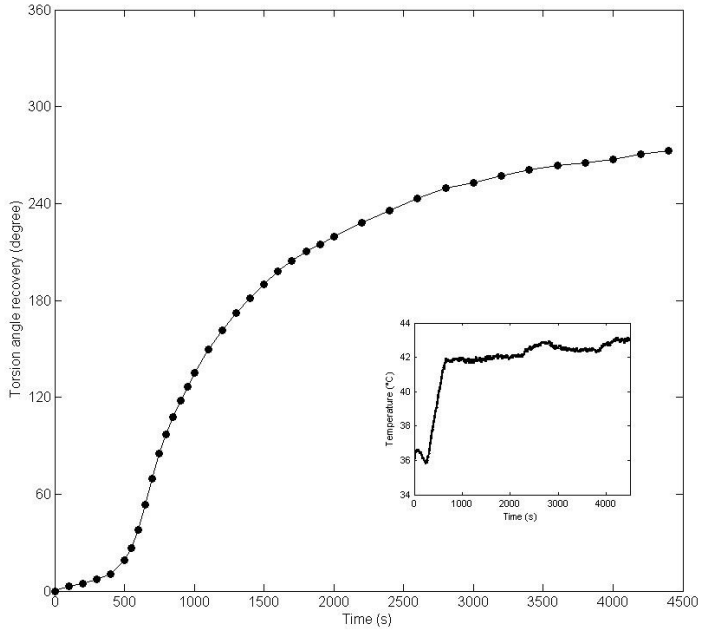

Fig. 5. Torsion shape recovery of the epoxy as a function of time when heating to 42 °C (< T_g) and holding isothermally at 42 ^{o}C.

3. Modeling

3.1 Thermoviscoelastic behavior

The amorphous thermoset under investigation was modeled using a generalized Maxwell model to describe its viscoelastic behavior obtained by experimental DMA data and a time-temperature superposition principle (Figure 3). The Maxwell model parameters were determined from the

storage modulus master curve, $G'(2\pi f)$, where f is the frequency. Validation of the model was performed on the loss angle (tan δ) master curve.

First, a value of the shear modulus at high temperature (G_e) (alternatively, low frequency) was selected at 1.6 MPa; a value slightly lower than the smallest value measured from the master curve. Thereafter, a suitable series of relaxation times and relaxation moduli (τ_i, G_i, respectively) pairs such that $G' = G_e + \sum_{i=1}^{n} G_i \frac{(2\pi f \tau_i)^2}{1+(2\pi f \tau_i)^2}$ remained to be defined. This is a classical problem in the rheology of amorphous polymers, and the procedure introduced by Weese (1993) was used here. It prevented the usual problems that incur from using a mere least square fit of the G_i values for a given set of τ_i values (e.g., negative G_i values). The ill-posedness of the problem is taken into account and treated using a Tikhonov regularization method, which in fact enforces a smooth fit of the master curve. The overall procedure provided very stable spectra when the number of regularly spaced τ_i's was varied. The NLREG (nonlinear regularization) program used to implement the procedure was disclosed by J. Weese and is available electronically from the World Wide Web. When applied to the $G'(2\pi f)$ data set measured, which extends over eight decades of logarithmic frequency scale, a series of twelve (τ_i, G_i) pairs was obtained. Their values are listed in Table 1 and plotted in Figure 6. A good fit can be observed in Figure 7a. Moreover, the same values agreed well with the predicted loss angle master curve, as shown in Figure 7b, which validated the fitting process used. It is emphasized that using a smaller number of (τ_i, G_i) pairs would lead to an incomplete description of the time-temperature behavior of the material, resulting in an inaccurate prediction of the shape-memory effect. This is accepted as a feature of the material considered, which is easily handled by standard identification procedures as explained above, and which is afforded by finite element codes. In summary, the thermoviscoelastic shear response of the epoxy was modeled using a generalized Maxwell model which parameters are listed in Table 1. The model was combined with the WLF equation (i.e., time-temperature dependence) which parameters are provided in section 2.2.

Additionally, in the pressure and temperature ranges considered here, it is reasonable to assume a purely elastic bulk modulus (i.e., no significant viscous effect). Both the small strain behavior of the material at low temperature (with ν = 0.38 in the glassy state, Smith et al. 1974) and its finite strain behavior at high temperature (with $\nu \approx 0.5$) could be covered by combining a constant bulk modulus of about 3.1 GPa with the high glassy ($G_g = G_e + \sum_{i=1}^{n} G_i$= 0.79 GPa) and low rubbery (G_e=1.6 MPa) shear moduli. Although as shown below this simple assumption gives very accurate results, the viscous volume effects or temperature-dependent bulk modulus values, as described by Ferry (1980) for instance, could be included without difficulty if necessary. Finally, the coefficients of linear thermal expansion were measured by thermal mechanical analysis at 5.7 10^{-5} °C^{-1} in the glassy state and to 2.44 10^{-6} °C^{-1} in the rubbery state.

Table 1.Generalized Maxwell model relaxation times and associated shear moduli pairs for the epoxy.

τ_i (s)	0.3031×10^{-4}	0.1721×10^{-3}	0.9768×10^{-3}	0.5545×10^{-2}	0.3147×10^{-1}	0.1787
G_i (Pa)	0.1476×10^{9}	0.1756×10^{9}	0.2025×10^{9}	0.1775×10^{9}	0.6802×10^{8}	0.1139×10^{8}
τ_i (s)	0.1014×10^{1}	0.5757×10^{1}	0.3268×10^{2}	0.1855×10^{3}	0.1053×10^{4}	0.5977×10^{4}
G_i (Pa)	0.2264×10^{7}	0.8132×10^{6}	0.4020×10^{6}	0.1760×10^{6}	0.5056×10^{5}	0.1265×10^{5}

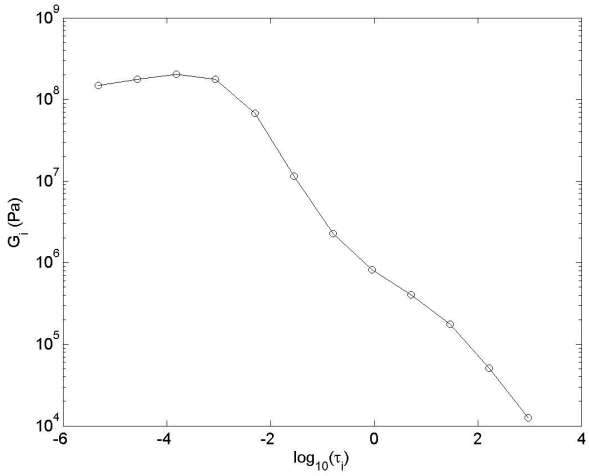

Fig. 6. Relaxation time spectrum calculated for the epoxy.

a) b)

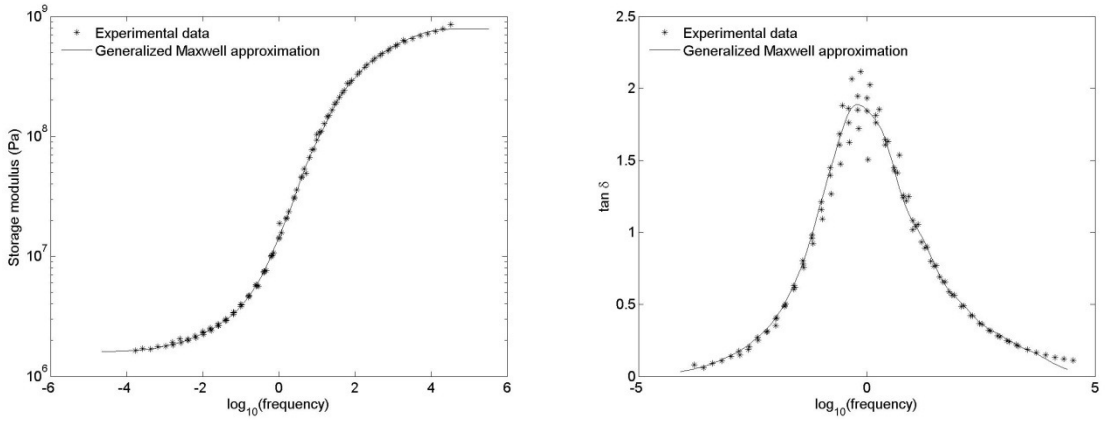

Fig. 7. (a) Comparison of the storage modulus master curves of the epoxy obtained experimentally and identified using a generalized Maxwell model with 12 relaxation times. (b) Validation of the model on the tan δ master curve of the epoxy obtained from time-temperature superposition.

3.2. Finite element simulations

Finite element simulation was used to implement the proposed model. Both the generalized Maxwell model and the WLF equation are available in the Abaqus standard (2010) finite element code (version 6.9). The finite strain extension of the generalized Maxwell model given by Simo (1987) is also included in the code, which can use the same relaxation times and shear moduli pairs that define the master curve for small strains. This provides an immediate extension of the model to finite strain and large deformation. In addition, a reference elastic behavior is required. In order to account for large deformation, a hyperelastic neo-Hookean model has been tested, which appeared to give an excellent agreement with the uniaxial tests that were performed up to 50% extension at high temperatures above T_g.

The 90 x 10 x 1.6 mm^3 deformable part (out of clamp) of the torsion specimen was meshed with 50 x 10 x 4 = 2000 8-node linear brick hybrid elements, which allowed a nearly incompressible behavior. The upper end of the mesh was fixed while the nodes of the lower end of the mesh were allowed to rotate together about the long axis of the specimen as a rigid solid; however they were not allowed to translate along this axis when the specimen was rotated by 360° at high temperature and subsequently cooled down to a low temperature. In contrast, they were allowed to both rotate and translate when the axial force on the specimen was released (Step 4) and during subsequent heating and shape recovery (Step 5, shape recovery). In step 4, this led to a contraction of the mesh along the long axis associated with the shape fixity. It may be noted that the actual temperature history recorded during the test was prescribed during the simulation of shape recovery. The complete simulation of the torsion shape-memory cycle was run in about 20 minutes on a laptop computer. Various stages of the computed mesh shape recovery are illustrated in Figure 8. At the end of Step 2 (torsion at high temperature), except near clamps and along edges, the strain state is close to simple shear, with a max value of 5.8% (11.6% engineering strain) at the surface of the specimen.

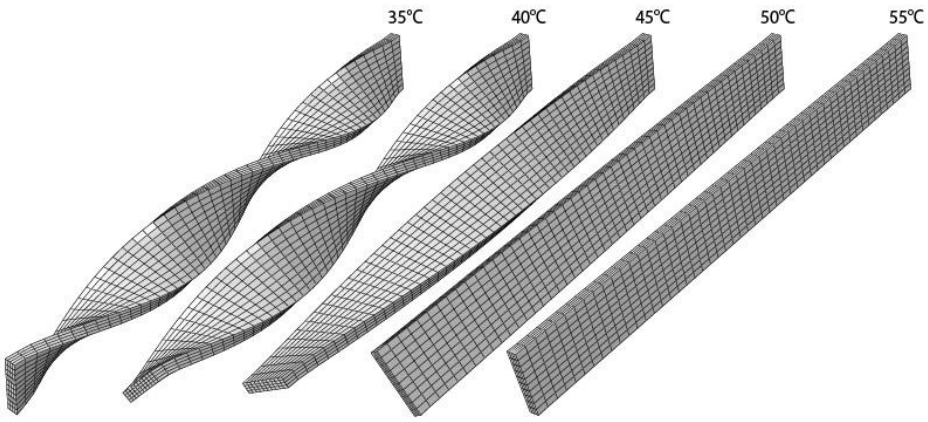

Fig. 8. Finite element simulation of the torsion shape recovery of the sample representative mesh when heated at 1 °C/min after a 360 ^{o} deformation.

3.3. Results

Simulations were run under identical conditions to those of temperature and deformation used experimentally (see section 2.3). Due to the sample thin thickness and the relatively slow heating rates considered here, we did not account for thermal conduction but merely applied the temperature on each node of the mesh. The bulk modulus and the coefficient of linear thermal expansion were found to have a negligible impact on the simulation results. This was expected since the deformation conditions involved mostly shear and no specimen length constraint.

Figure 9 shows the comparison between the simulation results and the experimental data for the torsion recovery of the material as a function of the heating rate. The simulation results and the experimental data are in very good agreement. Without adding any adjustable parameter, in contrast to many of the models previously reported and briefly discussed in the introduction, the model captures accurately the time and temperature-dependent torsion recovery. Most importantly, none of the previously reported models have shown comparable results as those presented here where such a good agreement between the shape memory behavior simulation and experimental data is evidenced.

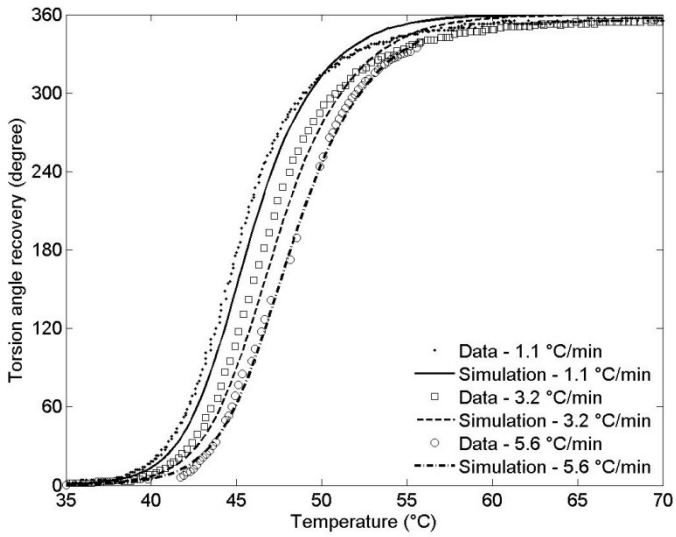

Fig. 9. Model simulation results and experimental data of the shape recovery process for the epoxy under varying heating rate.

In general, the material recovery is extremely sensitive to the temperature within the glass transition region. For the ramp-stop test, we measured an average temperature gradient along the

sample length of 1.0°C, therefore the average temperature along the sample was used for simulation purposes. Figure 10 shows the comparison between the experimental data and the simulation results for the ramp-stop test at 42 ^{o}C. Again, the model is in excellent agreement with the experimental shape recovery data.

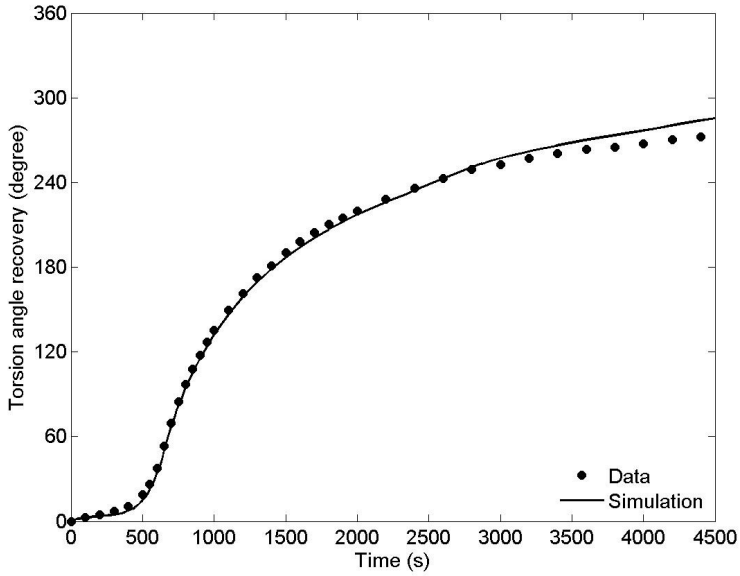

Fig. 10. Model prediction of the shape recovery as a function of time during 'ramp-stop' test at 42°C for the epoxy.

These results prove that the shape storage/shape recovery of amorphous polymer networks results only from their linear viscoelasticity and time-temperature-dependent behavior. For this class of polymers, a two-phase elastic model that considers the co-existence of a glassy phase and a rubbery phase is irrelevant. In fact, the present results show that the viscous nature of the polymer is essential to the shape memory effect with a deformation being stored as viscous strain owing to a large increase in viscosity (or equivalently in relaxation times) when the temperature decreases, and a shape being recovered (deformation released) when the viscous strain is released owing to a decrease in viscosity when the temperature increases. Therefore, interestingly, only using easily obtainable intrinsic material properties suffices to predict the shape storage/shape recovery properties of amorphous polymer networks. Note that, in contrast to Nguyen et al. (2008) and Srivastava et al. (2010) for instance, the simulation procedures reported here used built-in features of a commercial finite element code, hence neither extensive computational skills nor additional programming were required to accurately and precisely predict the shape memory behavior.

4. Conclusion

During the past decade, several, more or less complex models have been proposed to simulate the thermomechanical behavior of shape memory polymers. Their performances ranged from poor to fair despite their resort to either increasing the number of model parameters or introducing adjustable (i.e., fitted on shape-memory experiments) parameters,.

Here, an amorphous polymer network was submitted to large deformation torsion tests for shape storage/shape recovery under varying thermal histories to emphasize the time and temperature dependencies of the shape recovery. The thermomechanical behavior of the material was measured by dynamic mechanical analysis and implemented in the Abaqus finite element code in order to reproduce the shape memory cycling tests. The finite element simulations showed very good agreement with the experimental data, thereby demonstrating the time and temperature dependencies of the shape recovery of amorphous polymer networks. This is rationalized as a direct and sole consequence of the SMP's intrinsic viscoelasticity and time-temperature-dependent behavior. Therefore, traditional DMA characterization in deviatoric loading conditions enabled predicting precisely the shape recovery of the amorphous polymer network as a function of time and temperature. In fact, the overall shape recovery behavior was accurately simulated and predicted. Note that an accurate prediction of the shape recovery under loading conditions such as uniaxial tension or compression remains to be explored. Note also that the model predicts a (small) reaction torque if rotation is prevented during heating, or a force in uniaxial tests with fixed length, which still has to be compared to accurate experimental measurements. Although the proposed model was developed and validated only in the case of amorphous polymer networks, it is likely that similar models could be developed for other shape memory polymers, which are intrinsically viscoelastic materials with time-temperature-dependent properties.

Acknowledgements

This work was supported by the French “Agence Nationale de la Recherche” through project REFORM 10-JCJC-0917.

References

Abaqus/Standard, 2010. Dassault Systèmes Simulia Corp., Providence, RI, USA.
Castro, F., Westbrook, K.K., Long, K.N. , Shandas, R., Qi, H.J., Effects of thermal rates on the thermomechanical behaviors of amorphous shape memory polymers. Mech Time-Dependend Mater. (2010) 14, 219-241.
Chen, Y.C., Lagoudas, D.C., 2008a. A constitutive theory for shape memory polymers. Part I: Large deformations. J. Mech. Phys. Solids 56, 1752-1765.
Chen, Y.C., Lagoudas, D.C., 2008b. A constitutive theory for shape memory polymers. Part II: A linearized model for small deformations. J. Mech. Phys. Solids, 56, 1766-1778. Diani, J., Liu, Y., Gall, K., 2006. Finite strain 3D thermoviscoelastic constitutive model for shape memory polymers. Polym. Eng. Sci., 46, 484-492.Diani, J., Fredy, C., Gilormini, P., Merckel, Y., Régnier, G., Rousseau, I., 2011. A torsion test for the study of the large deformation recovery of shape memory polymers. Polym. Test. 30, 335-341.
Ferry, JD. Viscoelastic Properties of Polymers, 3rd ed. Wiley, 1980.
Gilormini P., Diani J., 2012. On modeling shape memory polymers as elastic two-phase composite materials. CR Mécanique to appear.
Heuchel, M., Cui, J., Kratz, K., Kosmella, H., Lendlein, A., 2010. Relaxation based modeling of tunable shape recovery kinetics observed under isothermal conditions for amorphous shape-memory polymers. Polymer 51, 6212-6218.
Hong, S.J., Yu, W.R., Youk J.H., Cho, Y.R., 2007. Polyurethane smart fiber with shape memory function: Experimental characterization and constitutive modeling. Fiber Polym. 8, 377-385.
Qi, H.J. , Nguyen, T.D., Castro, F., Yakacki, C.M., Shandas, R., 2008. Finite deformation thermo-mechanical behavior of thermally induced shape memory polymers. J. Mech. Phys. Solids 56, 1730-1751.
Lin, J.R., Chen, L.W., 1999. Shape-memorized crosslinked ester-type polyurethane and its mechanical viscoelastic model. J. Appl. Polym. Sci. 73, 1305-1319.
Liu, Y., Gall, K., Dunn, M.L., Greenberg, A.R., Diani, J., 2006. Thermomechanics of shape memory polymers: uniaxial experiments and constitutive modeling. Int. J. Plast. 22, 279-313.
Morshedian, J., Khonakdar, H.A., Rasouli, S., 2005. Modeling of shape memory induction and recovery in heat-shrinkable polymers. Macromol. Theory Simul. 14, 428-434.Nguyen, T.D., Qi, H.J., Castro, F., Long, K.N., 2008. A thermoviscoelastic model for amorphous shape memory polymers: Incorporating structural and stress relaxation. J. Mech. Phys. Solids 56, 2792-2814.
Reese, S., Böl, M., Christ, D., 2010. Finite element-based multi-phase modeling of shape memory polymer stents. Comput. Methods Appl. Mech. Eng. 199, 1276-1286.
Rousseau, I.A., Xie, T., 2010. Shape memory epoxy: Composition, structure, properties and shape

memory performances. J. Mater. Chem. 20, 3431-3441.
Simo, J.C., 1987. On a fully three-dimensional finite strain viscoelastic damage model: formulation and computational aspects. Comput. Methods Appl. Mech. Eng. 60**,** 153-173.
Smith, A., Wilkinson, S.J., Reynolds, W.N., 1974. The elastic constant of some epoxy resin. J. Mater. Sci. 9, 547-550.
Srivastava, V., Chester, S.A., Anand, L., 2010.Thermally actuated shape-memory polymers: experiments theory, and numerical simulations. J. Mech. Phys. Solids 58, 1100-1124.
Tobushi, H., Hashimoto, T., Hayashi, S., Yamada, E., 1997. Thermomechanical constitutive modeling in shape memory polymer of polyurethane series. J. Intell. Mater. Syst. Struct. 8, 711-718.
Wang, Z.D., Li, D.F., Xiong, Z.Y., Chang, R.N., 2009. Modeling thermomechanical behaviors of shape memory polymer. J. Appl. Polym. Sci. 113, 651-656.
Weese, J., 1993. A regularization method for nonlinear ill-posed problems. Comput. Phys. Commun. 77, 429-440.
Williams, M.L, Landel, R.F. and Ferry, J.D., 1955. The temperature dependence of relaxation mechanisms in amorphous polymers and other glass-forming liquids. J. Amer. Chem. Soc. 77, 3701-3707.
Xu,W., Li, G., 2010. Constitutive modeling of shape memory polymer based self-healing syntactic foam. Int. J. Solids Strctures 47, 1306-1316.